Revised Late Oligocene to Early Miocene magnetic stratigraphy recorded by drift sediments at Sites U1405 and U1406, IODP Expedition 342 (Newfoundland, NW Atlantic)

Tim E. van Peer[1]*, Chuang Xuan[1], Peter C. Lippert[2], Diederik Liebrand[1], Paul A. Wilson[1]

[1] Ocean and Earth Science, National Oceanography Centre Southampton, University of Southampton, Southampton, United Kingdom
[2] Dept. of Geology & Geophysics, Univ. of Utah, Salt Lake City, United States of America

* T.E.vanPeer@soton.ac.uk

Introduction

- Oligocene-Miocene Transition (OMT) is characterised by the "Mi1-event" (Transient oxygen isotope excursion) and carbon isotope shift.
- This represents transient ice sheet expansion and global cooling. It is considered to be astronomically forced by low amplitude variations in eccentricity and obliquity (Zachos *et al.*, 2001).

- The Oligocene-Miocene Boundary (OMB) is formally defined by reversal C6Cn.2r/C6Cn.2n at ~23 Ma.
- Therefore the recognition of the three C6Cn subchrons is crucial for locating the OMB and Mi1-event.
- We attempt to refine the Geomagnetic Polarity Time Scale (GPTS) by testing the putative identification of Late Oligocene to Early Miocene cryptochrons (Channell *et al.*, 2013).

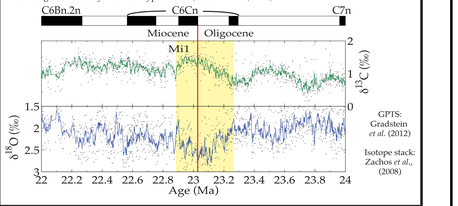

Background

- IODP Expedition 342 ("Paleogene Newfoundland sediment drifts") was drilled in the NW Atlantic (Norris, Wilson, Blum *et al.*, 2014a).

- Unprecedented opportunity to study the history of the Deep Western Boundary Current and Cenozoic climate change in the North Atlantic due to excellent foraminiferal preservation.

- Recovered grey-green nannofossil oozes deposited at high linear sedimentation rates (e.g. 2-4 cm/kyr at Site U1406 during the Late Oligocene to Early Miocene; 10-25 cm/kyr at Site U1405 across the Oligocene-Miocene Transition);

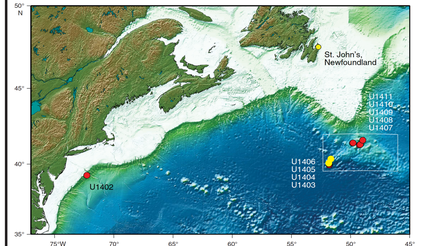

Norris, Wilson, Blum *et al.*, 2014a

Material & Methods

- U-channels samples (Tauxe, 1983) were taken from the prestine centre of 132 core sections (~190 m) of Site U1406 and 106 core sections (~138 m) of Site U1405.
- Magnetisation of all u-channel samples was measured on the narrow-bore superconductive rock magnetometer at the University of Southampton, which is optimised for u-channel measurements.
- NRM directions were calculated using Principal Component Analysis (PCA, Kirschvink, 1980) ranging 20-60 mT as incorporated in UPmag (Xuan and Channell, 2009).
- FlexIT tool data (Norris, Wilson, Blum *et al.*, 2014b and 2014c) were used to rotate declination directions of all three holes of Site U1405 and Holes A and B of Site U1406. The declination directions of Hole U1406C are rotated by calculating the circular mean of carefully selected normal (reversed) intervals. Subsequently, each core is rotated to 0° (180°).
- Eighty (80) First Order Reversal Curves (FORCs) were generated for each of the FORC diagrams. These FORCs were processed using the FORCinel (Harrison & Feinberg, 2008) and VARIFORC (Egli, 2013) software, with a smoothing factor (SF) of 5.

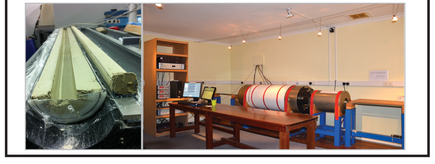

Results - U1405

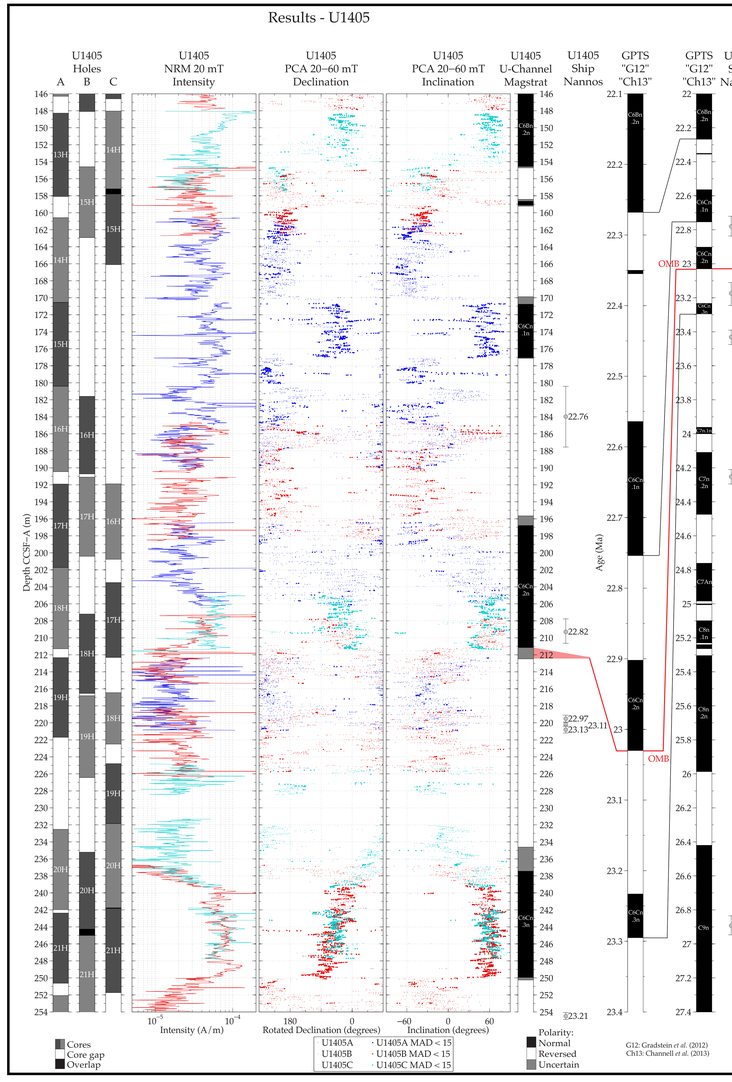

U1405A	· U1405A MAD < 15
U1405B	· U1405B MAD < 15
U1405C	· U1405C MAD < 15

Results - U1406

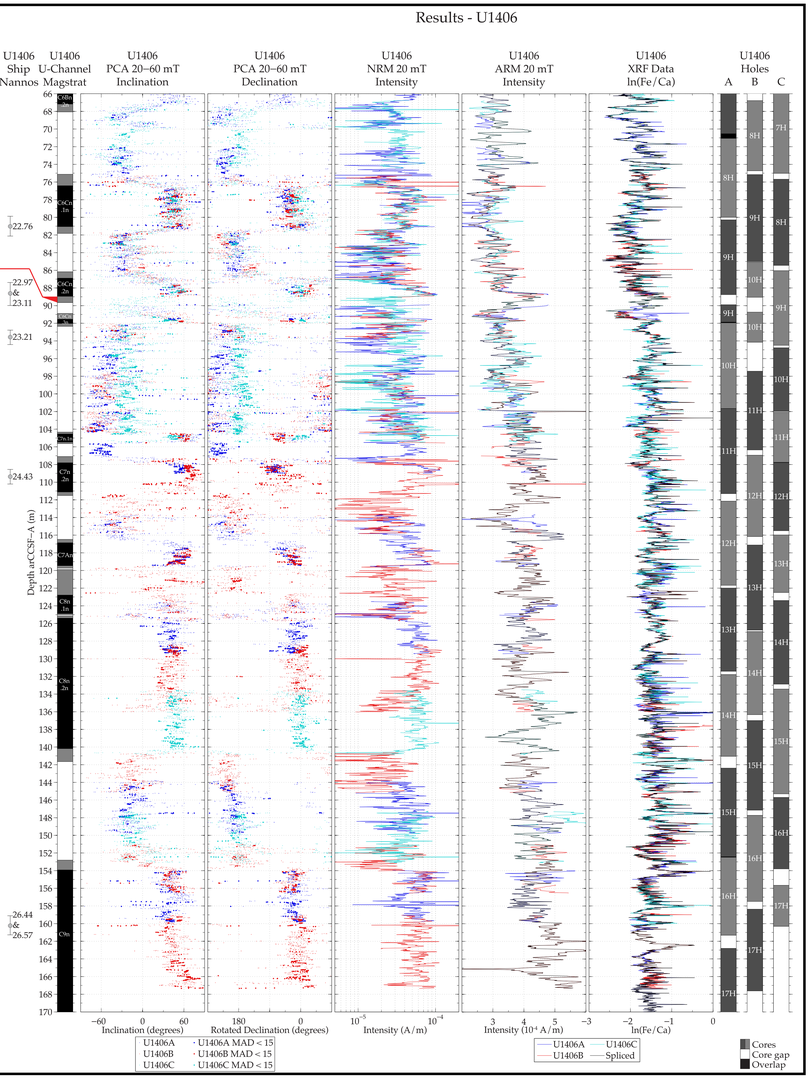

U1406A	· U1406A MAD < 15
U1406B	· U1406B MAD < 15
U1406C	· U1406C MAD < 15

U1406A	U1406C
U1406B	Spliced

Results - Zijderveld Diagrams and Preliminary Rock Magnetic Analyses

Orthogonal projection of the representative magnetic vectors on vertical (red circles) and horizontal (blue squares) planes.
All diagrams are plotted in sample (unrotated) coordinates.

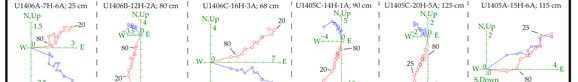

U1406B-11H-6W; 35 cm

Right: FORC diagram (see Methods).
Below: Low temperature Field Cooled (FC), Zero Field Cooled (ZFC) and Room Temperature (RT) remanences on warming and cooling. A subdued Verwey transition is visible in the RT remanence.

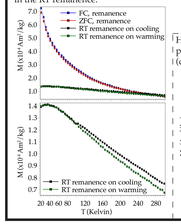

Hysteresis loops at different temperatures; adjusted for the ceramic (diagmagnetic) holder

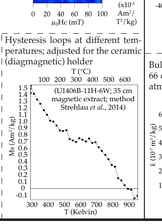

Bulk sample U1406B-10H-3W; 66 cm

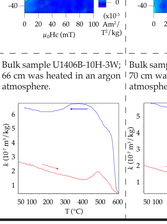

Bulk sample U1406B-10H-3W; 70 cm

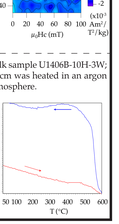

Bulk sample U1406B-10H-3W; 66 cm was heated in an argon atmosphere.

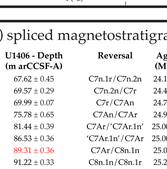

Bulk sample U1406B-10H-3W; 70 cm was heated in an argon atmosphere.

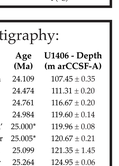

U1405 and U1406 u-channel (adjusted revised) spliced magnetostratigraphy:

Reversal	Age (Ma)	U1405 - Depth (m CCSF-A)	Reversal	Age (Ma)	U1406 - Depth (m arCCSF-A)	Reversal	Age (Ma)	U1406 - Depth (m arCCSF-A)
C6Bn.2n/C6Br	22.268	154.64 ± 0.08	C6Bn.2n/C6Br	22.268	67.62 ± 0.45	C7n.1r/C7n.2n	24.109	107.45 ± 0.35
C6Br/'C6Br.1n'	22.350*	158.54 ± 0.11	C6Br/'C6Br.1n'	22.350*	69.57 ± 0.29	C7n.2n/C7r	24.474	111.31 ± 0.20
'C6Br.1n'/C6Br	22.355*	159.17 ± 0.06	'C6Br.1n'/C6Br	22.355*	69.99 ± 0.07	C7r/C7An	24.761	116.67 ± 0.20
C6Br/C6Cn.1n	22.564	170.32 ± 0.44	C6Br/C6Cn.1n	22.564	75.78 ± 0.65	C7An/C7Ar	24.984	119.60 ± 0.14
C6Cn.1n/.1r	22.754	177.09 ± 0.04	C6Cn.1n/.1r	22.754	81.44 ± 0.39	C7Ar/C7Ar.1r	25.000*	119.96 ± 0.08
C6Cn.1r/.2n	22.902	196.22 ± 0.57	C6Cn.1r/.2n	22.902	86.53 ± 0.36	C7Ar.1n/C7Ar	25.005*	120.67 ± 0.21
C6Cn.2n/.2r	23.030	211.82 ± 0.67	C6Cn.2n/.2r	23.030	89.31 ± 0.36	C7Ar/C8n.1n	25.099	121.35 ± 1.45
C6Cn.2r/.3n	23.233	236.04 ± 1.42	C6Cn.2r/.3n	23.233	91.22 ± 0.33	C8n.1n/C8n.1r	25.264	124.95 ± 0.06
C6Cn.3n/C6Cr	23.295	250.11 ± 0.15	C6Cn.3n/C6Cr	23.295	92.19 ± 0.16	C8n.1r/C8n.2n	25.304	125.28 ± 0.13
			C6Cr/C7n.1n	23.962	104.43 ± 0.10	C8n.2n/C8r	25.987	140.92 ± 0.74
			C7n.1n/C7n.1r	24.000	105.55 ± 0.09	C8r/C9n	26.420	153.37 ± 0.56

* Cryptochrons 'C6Br.1n' and 'C7Ar.1n' are not incorporated in Gradstein *et al.* (2012); ages are rough approximations from data by Channell *et al.* (2013)

Summary

The U1405 and U1406 c-channel 20-60 mT PCA directions are charachterised by clear clusters of positive (negative) inclination and 0° (180°) declination. These normal (reversed) subchrons form a complete Late Oligocene to Early Miocene magnetic stratigraphy, deposited at relatively high sedimentation rates (U1406: ~2-4 cm/kyr; U1405: ~10-25 cm/kyr).
The subdued Verwey transition and Curie temperatures of ~250 °C and ~590 °C suggest that both magnetite and maghemite are present. The disentanglement of the relative contributions of maghemite and magnetite to the CRM will require further analyses.
In Chrons C6Br and C7Ar we also putatively identify a cryptochron. Channell *et al.*, 2013 previously identified both cryptochrons in the equatorial Pacific, and we therefore recommend that these will be incorporated into the future GPTS.

Future Work

- More rock magnetic analyses on both bulk samples and magnetic extracts to determine the relative contributions of maghemite and magnetite.

- Late Oligocene to Early Miocene astronomical tuning

- Full ARM, χ and IRM for environmental magnetic analysis

Acknowledgements

The Integrated Ocean Drilling Program (IODP) provided data and samples. IODP is sponsored by the U.S. National Science Foundation and participating countries under the management of Joint Oceanographic Institutions, Inc. The authors thank the IODP Expedition 342 Captain, crew and shipboard scientists. We thank Walter Hale, Alex Wülbers and Melanie Siegburg for their assistance with the u-channel sampling and Peter Blum, Rosanna Greenop, Wendy Kordesch, Dominik Leonhardt and Nevin Blum for the XRF core scanning. We acknowledge the financial support by NERC, UKIODP and an IRM Visiting Fellowship Grant.

Bibliography

Channell, J. E. T., C. Xhuxhuni, Y. Yamamoto, and M. S. Kesler (2013), Oligocene-Miocene magnetic stratigraphy carried by biogenic magnetite at sites U1334 and U1335 (equatorial Pacific, Ocean), *Geochemistry, Geophys. Geosystems*, 14(2), 265–282, doi:10.1029/2012GC004429.

Egli, R. (2013), VARIFORC: An optimized protocol for calculating non-regular first-order reversal curve (FORC) diagrams, *Glob. Planet. Change*, 110, 302–320, doi:10.1016/j.gloplacha.2013.08.003.

Gradstein, F. M., J. G. Ogg, M. Schmitz, and G. Ogg (2012), The Geologic Time Scale, Elsevier B.V., Amsterdam.

Harrison, R. J., and J. M. Feinberg (2008), FORCinel: An improved algorithm for calculating first-order reversal curve distributions using locally weighted regression smoothing, *Geochemistry, Geophys. Geosystems*, 9(5), Q05016, doi:10.1029/2008GC001987.

Kirschvink, J. L. (1980), The least-squares line and plane and the analysis of palaeomagnetic data, *Geophys. J. R. Astron. Soc.*, 62(3), 699–718.

Norris, R. D., Wilson, P.A., and Blum, P. *et al.* (2014a), Expedition 342 Summary, Proc. Integr. Ocean Drill. Progr., 342, doi:10.2204/iodp.proc.342.101.2014.

Norris, R. D., Wilson, P.A., and Blum, P. *et al.* (2014b), Site U1405, Proc. Integr. Ocean Drill. Progr., 342, doi:10.2204/iodp.proc.342.106.2014.

Norris, R. D., Wilson, P.A., and Blum, P. *et al.* (2014c), Site U1406, Proc. Integr. Ocean Drill. Progr., 342, doi:10.2204/iodp.proc.342.107.2014.

Strehlau, J. H., L. A. Hegner, B. E. Strauss, J. M. Feinberg, and R. L. Penn (2014), Simple and efficient separation of magnetic minerals from speleothems and other carbonates, J. Sediment. Res., 84, 1096–1106, doi:10.2110/jsr.2014.89.

Tauxe, L., J. L. LaBrecque, R. Dodson, M. Fuller, and J. DeMatteo (1983), U-channels - A new technique for paleomagnetic analysis of hydraulic piston cores, in *Eos, Transactions American Geophysical Union* 64, p. 219, San Francisco.

Xuan, C., and J. E. T. Channell (2009), UPmag: MATLAB software for viewing and processing u channel or other pass-through paleomagnetic data, *Geochemistry, Geophys. Geosystems*, 10, Q10Y07, doi:10.1029/2009GC002584.

Zachos, J. C., N. J. Shackleton, J. S. Revenaugh, H. Pälike, and B. P. Flower (2001), Climate response to orbital forcing across the Oligocene-Miocene boundary, *Science*, 292, 274–278, doi:10.1126/science.1058288.

Zachos, J. C., G. R. Dickens, and R. E. Zeebe (2008), An early Cenozoic perspective on greenhouse warming and carbon-cycle dynamics, *Nature*, 451(7176), 279–283.